Carbohydrate Polymers 108 (2014) 272–280

Contents lists available at ScienceDirect

Carbohydrate Polymers

journal homepage: www.elsevier.com/locate/carbpol

Polybutylene succinate adipate/starch blends: A morphological study for the design of controlled release films

Fadi Khalil, Sophie Galland, Amandine Cottaz, Catherine Joly*, Pascal Degraeve

Université de Lyon, Université Lyon 1-ISARA Lyon, Laboratoire de Bioingénierie et Dynamique Microbienne aux Interfaces Alimentaires (BioDyMIA, EA n°3733), IUT Lyon 1 site de Bourg en Bresse, Technopole Alimentec, rue Henri de Boissieu, F-01000 Bourg en Bresse, France

ARTICLE INFO

Article history:
Received 16 December 2013
Received in revised form 18 February 2014
Accepted 19 February 2014
Available online 28 February 2014

Keywords:
Polymer blends
Morphology
Release
Migration
Permeation
Active packaging

ABSTRACT

Films made of plasticized starch (PLS)/poly(butylene succinate co-butylene adipate) (PBSA) blends were prepared by thermomechanical processing varying the PBSA proportions in blends to obtain biphasic materials with distinct morphologies. These morphologies were characterized by selective extraction of each phase, microscopic observations, and selective water/oxygen permeation properties. These experiments allowed identifying the blend compositions corresponding to the beginning of partial continuity (cluster partial percolation) until total continuity of each phases. This property was related to the controlled release of model molecule (fluorescein) previously dispersed in the PLS and revealed that its release depended on the tortuosity of the PLS phase tailored by the polymer blends composition and by the limited swelling of the PLS when entrapped in the PBSA phase. Future applications will focus on food preservatives dispersed in PBSA-PLS blends to obtain active antimicrobial packaging put in direct contact with intermediate to high moisture foods.

1. Introduction

To overcome the limitations of passive barrier prepared with conventional formulations, the development of controlled release materials presents a growing interest achieved by the incorporation of active compounds in polymer matrices. In food, cosmetic or pharmaceutical packaging, embedded molecules play an active role to preserve the properties of the packaged products. Meanwhile, in Europe, regulation on such active packaging limited the applications and research effort for a long time (Regulation EC no. 1935/2004, EC no. 450/2009) while in modern drug delivery, strategies to optimize the release profile of the active compounds were designed (Siepmann, Siepmann, Walther, MacRae, & Bodmeier, 2008).

Amongst the studied systems, immiscible polymers blends are promising ones when used as materials or coatings. As they are immiscible (or partially miscible), polymer blends usually lead to biphasic structures with evolving morphologies playing with their composition: matrix-dispersed particle structures, matrix-fiber structures, lamellar structures or co-continuous structures. Selective solvent extraction, microscopic observations and viscoelastic properties are usually used to investigate these blends (Castro, Carrot, & Prochazka, 2004, Schwach & Avérous, 2004). According to Pötschke and Paul (2003), the polymer blend morphology is based on the percolation concept. When the percolation occurs, one part or the totality of one of the two phases forms a continuous structure that permeates the whole sample and eventually dominates the properties of the blend. A distinction between partial continuous structures and full continuity can be made. When one phase is totally continuous, it can be traversed from side to side without crossing any interface. When the polymer phase is partially continuous, some sample areas are inaccessible (without crossing any interface).

Transport properties of such polymer blends are sensitive to changes in material morphology especially because of the percolation phenomenon which makes diffusion paths more or less tortuous (Leuenberger, Bonny, & Kolb, 1995; Romm, 2002). In fact, the blend morphology can be well investigated by permeation properties (Espuche, Escoubes, Pascault, & Taha, 1999). For example, Soney, Ninan, and Sabu (2001) studied the variation of gas permeability of membrane made of SBR (styrene butadiene rubber and natural rubber- i.e. NR-) with different volume fractions of natural rubber. They concluded that matrix-dispersed morphology makes tortuous path for the gaseous molecules until the dispersed phase (NR) becomes a continuous one and thereby enhances a sharp permeability increase. From theoretical and experimental

* Corresponding author. Tel.: +33 474472142; fax: +33 474455253.
E-mail address: catherine.joly@univ-lyon1.fr (C. Joly).

http://dx.doi.org/10.1016/j.carbpol.2014.02.062
0144-8617/

approaches, Park, Cohen, and Langer (1992) concluded on a drastic permeability increase at the percolation threshold where the minor component starts to make a continuous channel across the membrane. Other authors used partially miscible blends to successfully adjust drug diffusivity, or delivery of proteins (Lyu, Sparer, Hobot, & Dan, 2005) playing with the hydration properties to activate the diffusion.

Over the last decades, literature has focused on biodegradable or biosourced polymer blends (Auras, Harte, & Selke, 2004; Woodruff & Hutmacher, 2010; Yu, Dean, & Li, 2006) involving a renewable polymer and aliphatic polyesters (PCL, PLA, PHA, PBS, PBSA, etc.), studied to achieve better physical properties (mainly mechanical properties, water sensitivity, etc.). Amongst natural polymers, starch has been widely studied because it is suitable for plastic processing (extrusion or injection) when plasticized with both water and polyols (generally glycerol) (Averous & Boquillon, 2004; Rodriguez-Gonzalez, Ramsay, & Favis, 2006) to be called Plasticized Starch or PLS. Amongst the polyesters, polybutylene succinate (PBS) and copolymers (PBSA – i.e. poly(butylene succinate-co-butylene adipate) are noteworthy because of their intrinsic thermal properties located in between polypropylene and polyethylene ones, which are the synthetic polymers frequently used as packaging materials. Moreover, PBS and copolymers are nowadays synthesized from fossil resources but are expected to be "all green" in the future as monomers can be obtained by bacterial fermentation (Song & Lee, 2006).

In this work, several blends made from polar PLS and semi-polar PBSA have been investigated to study the possible relationships between blends morphology and the controlled release of migrants/probes used as model molecules. The applications, once morphology explained, will focus on dispersion of food preservatives in blends to design antimicrobial packaging materials.

The blends morphology was thus investigated by combining information resulting from:

(1) selective extraction of each phase enriched by microscopic observations
(2) selective transport properties of oxygen and water vapor through gas permeation experiments
(3) water sorption experiments (since transport can be modified/activated by water sorption of PLS)
(4) fluorescein desorption studies.

2. Materials and methods

A series of biphasic blends made of plasticized corn starch (30%wt. glycerol, on a dry matter basis) (PLS) manufactured by Clextral S.A. (Firminy, France) and PBSA, purchased from NaturePlast (Caen, France) were prepared as described below. For fluorescein desorption studies and confocal scanning laser microscopy observations, PLS was formulated with fluorescein sodium salt (Sigma–Aldrich, Saint Quentin Fallavier, France).

2.1. Blends preparation

Various PBSA/PLS blends (from 0 to 100 wt.% PBSA content, Table 1) were prepared from granules of each component. PLS granules were previously equilibrated at 50% RH and 23 °C until constant weight (i.e. for one week). The blends are denoted as follows: PBSA10 means that the blend contains 10% of PBSA and 90% of PLS. Two methods of blend preparation were used.

2.1.1. Melt blending

The melt blending was carried out in a Haake internal batch mixer Rheomix 600® (Thermo Scientific, Villebon sur Yvette, France). The mixing temperature was set to 120 °C. The roller speed was 50 rpm. The average shear rate was estimated to be 25 s^{-1}. After 10 min mixing, the torque was found to be constant.

2.1.2. Extrusion process

2.1.2.1. PLS/PBSA blends. Extrusion was performed by two runs in a three-zone single-screw extruder (Scamex, Crosne, France) (heated at 120, 120, and 110 °C, respectively). A fourth zone at 110 °C of a vertical downright annular die was added to prepare tubular extruded films. The rotation speed of the extruder screw was set at 50 rpm which gave an approximate residence time of ~55–60 s. The sample stands issued from the first run were pelletized (Scamex pelletizer, Scamex) and, as previously described, re-extruded to get a better homogeneity.

2.1.2.2. Labeled PLS/PBSA blends. PLS phase was labeled with fluorescein sodium salt at two concentrations: 50 and 500 ppm before blending with PBSA for two purposes. Fluorescein sodium salt was added to PLS for confocal scanning laser microscopy observations of the blends (fluorescein being a fluorescent probe for PLS phase visualization) and for the release study in water, respectively. The extrusion process was the same as described in the former paragraph but starch pellets were previously sprayed by an adequate amount of aqueous solution of fluorescein sodium salt. This amount was calculated to reach the global water uptake of starch corresponding to a storage at 50% RH (i.e. 9 wt.%) (Godbillot, Dole, Joly, Roge, & Mathlouthi, 2006) and needed for starch extrusion. Moreover, pellets were conditioned at 50% RH and 23 °C for one week before extrusion.

2.1.3. Samples conditioning

All the samples prepared either by melt blending or by extrusion were conditioned (50% RH and 23 °C for one week) before being characterized.

2.1.4. Films preparation

Samples from blends were pressed molded into films by using a constant thickness film maker mold placed in a hydraulic press equipped with platens heated at 120 °C (Specac, Eurolabo, Saint Chamond, France), a 4 ton pressure was applied for 20 s. The duration of fluorescein desorption kinetics, water sorption as well as oxygen and water vapor permeability measurement experiments depended on membrane thicknesses. Therefore films with different controlled thicknesses were prepared in order to get a suitable duration for these experiments and to limit the immobilization of corresponding instruments. Typical thicknesses were around 60 ± 10 μm for measurements of fluorescein desorption kinetics with a spectrofluorimeter, 230 ± 10 μm for water sorption in a climatic chamber and 330 ± 10 μm for gas permeation (O_2 and water vapor).

2.2. Blend morphology characterization

Selective solvent extraction and microscopic observations were combined for the evaluation of the blends morphology. Before and after extraction, as previously mentioned, sample pieces (1–2 g) have been conditioned for one week at 50% RH and 23 °C before weighing (especially after PBSA removal).

2.2.1. Solvent extraction

Extraction of each polymer phase by a selective solvent allowed quantifying its continuity index. Solvents have to be carefully chosen to dissolve or extract completely each phase without any influence on the second one. In this study, PBSA was dissolved in dichloromethane (99.9%, Chimie Plus, Denice, France) during 24 h whereas PLS was hydrolyzed in 6 mol L^{-1} HCl during 48 h (Sarazin, Li, Orts, & Favis, 2008; Schwach & Avérous, 2004). The extraction

Table 1
PBSA/PLS blends (the code is based on the PBSA percentage).

Code	PBSA0	PBSA10	PBSA20	PBSA30	PBSA35	PBSA40	PBSA45	PBSA50
PBSA (wt.%)	0	10	20	30	35	40	45	50
PLS (wt.%)	100	90	80	70	65	60	55	50

Code	PBSA55	PBSA60	PBSA65	PBSA70	PBSA80	PBSA90	PBSA100
PBSA (wt.%)	55	60	65	70	80	90	100
PLS (wt.%)	45	40	35	30	20	10	0

procedure was repeated 3 times to constant weight in a Soxhlet extraction apparatus for PBSA and directly in a beaker with a large excess of HCl solution at room temperature for PLS. After extraction, the samples were dried (70 °C, 48 h) and reconditioned (50% RH, 23 °C) as previously mentioned before weighing because of the starch hygroscopic properties.

Elsewhere, the distribution of glycerol between both phases had to be taken into account. Glycerol mass balance between extracted samples and solvent was analyzed by assaying glycerol by GC-FID (Clarus 500, Perkin Elmer, Courtaboeuf, France) using a RTX-WAX column (30 m–0.32 mm–0.25 μm) (Restek, Lisses, France). The continuity of one phase can be defined as the fraction of polymer that belongs to a continuous phase, which can be evaluated with the following expression (Eq. (1)):

$$\%\,\text{continuity of } i = \frac{(\text{weight of whole sample} - \text{weight of whole sample after extraction of } i) + \text{weight of extracted glycerol}}{(\text{weight of } i + \text{weight of glycerol}) \text{ in the sample before extraction}} \times 100 \quad (1)$$

2.2.2. Scanning electron microscopy (SEM)

After dissolution (or hydrolysis) of one phase in the appropriate medium, samples were examined with a Hitachi S3000-N Scanning Electron Microscope (Verrières-le-Buisson, France) at 5 kV accelerating voltage. The bulk and the material surface were observed.

2.2.3. Confocal laser scanning microscopy (CLSM)

The films made of PBSA70 were formulated with 50 ppm of fluorescein sodium salt and prepared by extrusion as previously described. CLSM observations were performed with a Zeiss LSM 510/Meta Axiovert 200 (Carl Zeiss, Marly le Roi, France) confocal laser scanning microscope (excitation at 488 nm (argon laser), detection Long Pass 505 nm filter, 40× objective/NA 1.3 oil (pinhole 1Unit Airy i.e. 1 μm optical section)). Transversal sections (15 μm thick) were prepared using an ultra-microtome. Just before the observation, water and a coverslip were added, and the preparation was sealed with nail varnish.

2.3. Oxygen and water permeation

Films (0, 30, 40, 50, 60, 65, 70, 80, and 100% PBSA, typical thicknesses around 330 ± 10 μm, preconditioned one week at 50% RH and 23 °C) were sealed between two aluminum foil masks, purchased from Lippke GmbH (Neuwied, Germany), leaving an uncovered film area of 5 cm^2. Araldite epoxy resin (Bostik, USA) was used to insure water tightness and air tightness at the contact zones between the films and the foil masks. All actual exchange surfaces after deposition of epoxy resins were recalculated by optical analysis (between 4.1 and 4.9 cm^2). Oxygen and water permeation measurements were performed on two different batches of samples (specific extrusion for each batch).

Oxygen transmission rates were determined at 23 °C and 50% RH using a Systech 8001 permeameter (Gruter et Marchand, Nanterre, France) equipped with a coulometric oxygen sensor. Samples were placed between the two compartments of a permeameter cell maintained respectively at 1 bar (upstream oxygen partial pressure), whereas the downstream compartment was swept by pure nitrogen (ASTM D-3985-81). Oxygen fluxes were recorded until the plateau value (steady state) and transformed in oxygen permeability coefficient units often used in literature (cm^3 μm/m^2 day atm) multiplying it by the film thickness in relevant units (μm). To convert (cm^3 μm/m^2 day atm) in SI units (mol/m s Pa), these values have to be multiplied by 5.28×10^{-21}, and by 10^{-2} to convert in cm^3 m/m^2 d kPa, respectively. Oxygen permeameter was periodically calibrated (inter-laboratory comparative testing) by Smithers Pira (Leatherhead, UK) (http://www.smitherspira.com/testing/material-properties/plastic/barrier-properties.aspx).

Water vapor (WVTR) transmission rates were determined at 23 °C and for a partial pressure gradient equal to 50–75% RH. WVTR were measured by the "wet cup method" as the water vapor fluxes were very high, placing the film sample of the tested blends over the top of a pre-made water tight metal cup. The cup contained a sodium chloride saturated aqueous solution and was placed in a climatic chamber (50%).

2.4. Water vapor sorption

Water sorption kinetics were determined by placing samples in a Vötsch (Week 0028 MI) climatic cell (Balingen, Germany) with controlled humidity and temperature. Water uptake was measured continuously with a Radwag electronic microbalance (Radom, Poland) located inside the cell and connected to a computer system. For each formulation, around 11 films (2–3 g) (each film having a diameter of 25 mm, a thickness of 230 ± 10 μm) previously conditioned at 45% RH and 20 °C until constant weight underwent a water vapor partial pressure increment from 45% to 75% RH.

The apparent diffusion coefficients (D_1) of water vapor were determined from the kinetics of water uptake data using the first Fick equation solution at short times ($w_t/w_\infty \leq 0.5$) (Eq. (2)):

$$D_1 = \frac{\pi \beta_1^2 e^1}{16} \quad (2)$$

- where e, the sample thickness and β_1, the slope of the beginning of the experimental curve $(W(t))/W_\infty = f(\sqrt{t})$ when linear
- where $W(t)$ is the sample weight as a function of time and W_∞ their weight at equilibrium.

Water uptakes (WU) at 45% and 75% RH at equilibrium were calculated after a film drying step for 48 h at 60 °C from the Eq. (3):

$$\%\text{WU} = \frac{W_h - W_d}{W_d} \times 100 \quad (3)$$

- where W_d and W_h are the weight of the dry and hydrated sample, respectively.

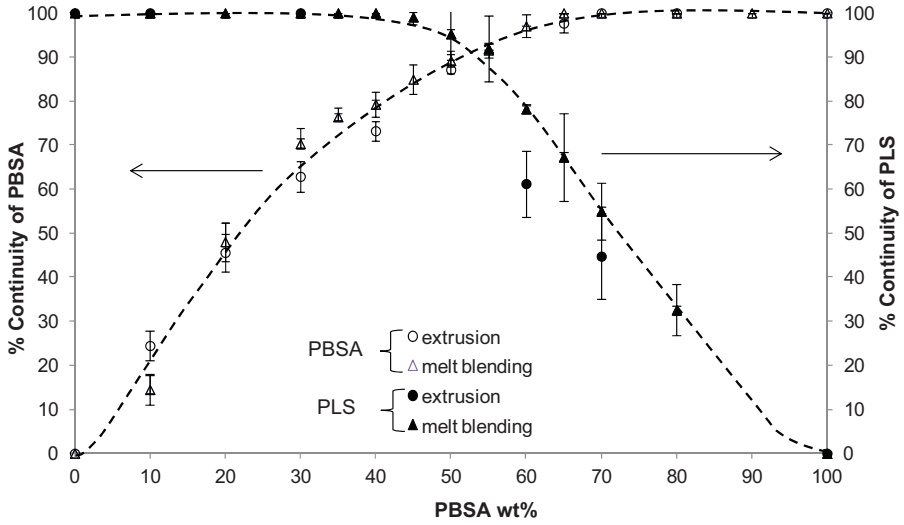

Fig. 1. Continuity diagram of PBSA (empty symbols) and PLS (full symbols) as a function of PBSA content. Influence of the elaboration process (melt blending or extrusion) on the extractability of each phase (percentage of extractible considered polymer) as a function of the blend composition.

2.5. Fluorescein desorption experiments

Desorption in water of fluorescein from formulated films was monitored with a LS 55 spectrofluorimeter (Perkin Elmer, France) at 22 °C. Films (thickness of $60 \pm 10\,\mu m$) were previously formulated with fluorescein sodium salt (500 ppm/PLS content as previously stated) before being properly shaped as disks of 8 mm diameter, suspended from a needle passing through the cap cell before being immersed in 4 mL distilled water placed into disposable polystyrene spectrofluorimeter cells. The desorption systems were glued with Araldite® epoxy resin (Bostik-USA) to prevent any water evaporation. All systems (cell + suspended film) were excited at 490 nm and the emission was recorded as a function of time at wavelengths depending on the chromophore concentration (between 540 and 590 nm) to avoid any saturation phenomenon and to have enough sensitivity at the first time of diffusion thanks to a four-position automatic cell changer. The apparent diffusion coefficients were calculated from the desorption kinetics curves using Eq. (2) (the linearity between the emission signal and the fluorescein concentration had been previously verified).

3. Results and discussion

Several compositions of PLS/PBSA blends were prepared and coded depending on the PBSA content mainly from PBSA 10 to PBSA 80 (Table 1). For example, PBSA10 was made of 10 wt.% PBSA + 90 wt.% PLS.

Two different processing methods were used to investigate the influence of the blend formulation on their morphology: an internal blender and a mono screw extruder (two runs). As PLS and PBSA are immiscible, biphasic blends were obtained whatever the processing method. Then, films with controlled thicknesses were prepared by thermoforming to study the impact of the blend formulation on the one dimension diffusion (1D) of migrants, paying attention to the potential evolution of the morphology induced by thermoforming.

3.1. Blend morphology study by selective extraction and imaging

3.1.1. Selective extraction

Selective extraction associated with microscopic observations is the basic analysis used to investigate the morphology of polymer blends (Castro, Prochazka, & Carrot, 2005). It consists in a gravimetric solvent extraction of the dispersed phase achieved by a suitable solvent (or reactant). This operation was performed for both phases (see Eq. (1)): PBSA was solubilized by dichloromethane, while starch was hydrolyzed in a concentrated HCl bath, as no suitable solvent for starch extraction is available.

Fig. 1 shows the continuity diagram for the two phases (PBSA and PLS) obtained from materials blocks (1–2 g). Both curves present the same shape giving the proportion of the dispersed polymer able to be extracted as a function of the PBSA proportion. As expected, the curves increase regularly until 100% when extractable polymer forms the continuous phase. This evolution occurs when one of the polymers (the minor component) is trapped by the second one (the major component) into a droplet/continuous phase morphology. The diagram shows no significant difference between the two methods of mixing used in this work (melt blending or extrusion) although melt blending was initially supposed to ensure better mixing. Several materials (from PBSA 30 to 70) were also extracted after a thermoforming step used to make films in order to verify if the continuity curves are the same whatever the materials shape (small blocks or films – 330 mm). For the three tested compositions, the points were superimposed (data not shown for clarity) to the PSA continuity curve, supposing an unchanged morphology. However, for the PLS curve, data were not reproducible enough to conclude clearly.

For the 10% to 20% PBSA blends, the PBSA phase is mainly dispersed in the PLS phase. Then between 20% and 60% PBSA, the PBSA phase begins to be partially continuous (partial nodules coalescence) presenting a continuity index superior to 50%. The full continuity of PBSA (100% continuity index (CI)) is reached above 55% PBSA taking into account the experimental error bar. This value will be interesting for the following transport properties study, since this also means that above 55% PBSA in blends, a continuous PBSA paths network is formed throughout the materials. Then, for the other curve, the majority of the PLS phase is dispersed (PLS nodules) in PBSA phase from 70% to 80% PBSA blends (20–30% PLS). For higher PLS contents, PLS begins to be partially continuous and the full PLS continuity seems to be reached for PBSA contents lower than 45–50%. From data in Fig. 1, no co-continuous morphology is noticeable when each phase presents simultaneously an overlapping with a percentage of continuity equal to 100% for both polymers (Galloway, Koester, Paasch, & Macosko, 2004; Li, Ma, & Favis, 2002; Pötschke & Paul, 2003). In the literature devoted to starch based blends, it is rare to find any continuity for PLS because

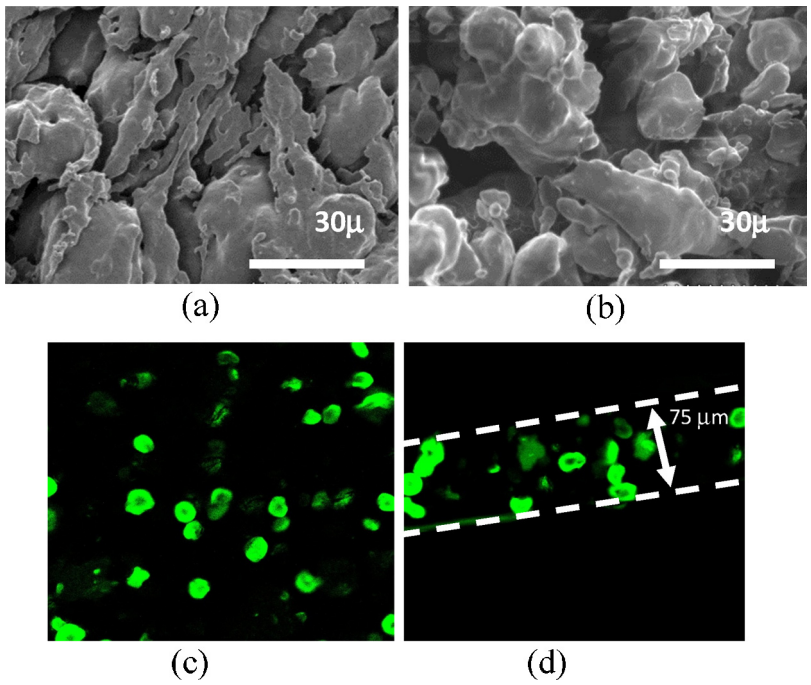

Fig. 2. SEM images of (a) PBSA30 and (b) PBSA60 after extraction with dichloromethane and CLSM observations of PBSA70 showing fluorescein-labeled PLS nodules (c) after extrusion (film thickness 320 μm) or (d) after extrusion and thermoforming (film thickness: 75 μm).

no suitable solvent is available for starch, as stated previously. For that reason, PLS phase underwent an acidic hydrolysis for 48 h. This step was difficult to manage and required optimization: when the hydrolysis lasted a longer time (72 h) the percentage for PLS was slightly over 100% (data not shown). This could only be explained by a partial degradation of the PBSA phase (ester bond hydrolysis) even if pure PBSA immersed in 6 mol L^{-1} HCl showed no significant weight decrease for the same duration. This could be explained by a difference in PBSA crystallinity rate (and thus PBSA acidic hydrolysis kinetics) as a function of the PLS content as already reported (Jbilou et al., 2013). Therefore, the PLS continuity curve (Fig. 1) was constructed with the data resulting from a 48 h hydrolysis in HCl. It can thus be considered as an approximation with probable slightly underestimated or overestimated values depending on blend composition and crystallinity rate of PBSA. Consequently, the global morphology of the blends is not completely elucidated by such a diagram of continuity (Fig. 1). For that reason, other investigations by techniques such as microscopic observations were also performed.

3.1.2. Scanning electron microscopy and confocal laser scanning microscopy

Fig. 2 presents the SEM images of 2 PBSA-PLS blends observed after extraction of the PBSA phase (PBSA30 and PBSA60, Fig. 2(a) and (b). In addition, PBSA70 blend films made from PLS phase previously labeled with fluorescein sodium salt (50 ppm) were observed by confocal laser scanning microscopy (CLSM).

The SEM images show the highly textured structure obtained for starch based phase (Fig. 2(a)) when PLS phase is 100% continuous. Indeed, the PLS matrix seems to be stretched to form further the expected network attempted for a future continuous phase (Fig. 2(b)). For this type of blend with 30% of PBSA (Fig. 2(a)), the continuity percentages of PBSA and of PLS are around 65% and 100%, respectively. Then, for 60% of PBSA (Fig. 2(b)), the continuity percentage of PBSA is roughly 100%. A macroscopic PBSA network seems to appear by percolation of the stretched nodules by mechanical shear stress. The CLSM observations show the nodular structure of the PBSA70 blends (Fig. 2(c)) obtained after the annular die and highlighted the conservation of this structure after thermoforming (Fig. 3(d)) (nodules). However, a partial nodule percolation would be noticeable probably induced by the drastic decrease in thickness from 320 to 75 μm.

As a conclusion of the selective extraction study completed by microscopic observations, no significant influence of the process of mixing used to make blends and of the materials shape (small blocks or films) seemed to be observed. Simple single screw extrusion can thus be used to prepare materials. Secondly, as expected, different morphologies can be achieved as already described from embedded nodules to partial continuity and to total phase continuity. These observations are consistent with the double curve shown on the continuity diagram (Fig. 1). In the context of controlled release materials, it is necessary to work with materials with a controlled shape. Films with controlled thicknesses were prepared by thermoforming at high temperature. Consequently, the question of the retention (stability) of the morphology of blends following this short thermoforming treatment had still to be addressed.

3.2. Indirect blends morphology study by transport property assessment

At this stage of the study, the blend morphology study was completed by assessing the transport properties (permeation, sorption and diffusion) of different molecules in order to state about the continuity of the two phases, the morphology stability, and the expected controlled release.

3.2.1. Oxygen and water vapor permeation

Gas permeation properties of films made of thermoformed PBSA/PLS blends were determined to quickly assess the transport properties and the interface quality between phases. Interface quality can be clearly assessed by this technique since “defects” lead generally to high and abnormal gaseous fluxes.

Oxygen and water vapor were used as selective apolar and polar probes, respectively, giving information on the continuity of each

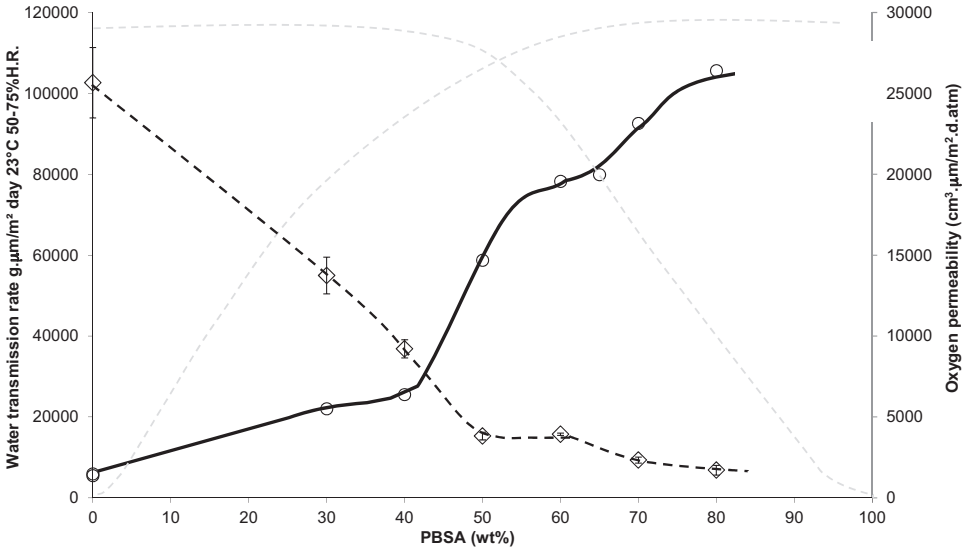

Fig. 3. Oxygen permeability and water vapor transmission rate as a function of the blend composition. Curves from Fig. 1 (gray lines) were added for correlation purposes.

phase. In fact, O_2 diffuses preferentially through the PBSA paths, whereas water molecules diffuse preferentially through the PLS ones. The results are displayed in Fig. 3. Oxygen and water vapor permeation fluxes are in good agreement with biphasic materials with two phases presenting a rather good adherence with permeation coefficient values in the range of those expected for each component (http://www.succipack.eu/; Dole, Joly, Espuche, Alric, & Gontard, 2004). As expected, the oxygen permeability of films made of PBSA/PLS blends increased with PBSA content, while the water vapor transmission rate decreased. Oxygen permeability as a function of PBSA content in blends presents a double S-shape with 2 significant discontinuities: the first increase is more important when PBSA contents increase from 40% to 55% than from 60% to 75%. This first discontinuity (starting at 40%) is probably due to the beginning of the PBSA nodules percolation inducing the possibility for O_2 to diffuse preferentially through the newly formed network structure (PBSA diffusion paths network) until a plateau value where the continuity index of PBSA phase reached 100%. The second discontinuity is attributed to a secondary percolation threshold taking place when the remaining disconnected small clusters start coalescing to form a continuous network. Conversely, the same behavior is observed for water vapor transmission rate of PLS phase. Water vapor fluxes decrease rapidly up to 50% PBSA content in blends and remain then quite constant from 50% to 80% PBSA content, except the slight event observed simultaneously to the secondary percolation phenomenon reported for the PBSA phase: the second discontinuity (which makes paths unavailable for water diffusion) is concomitant with the percolation of the remaining small PBSA clusters. It has to be noticed that these experiments have been made on two different batches of samples, from differentiated extrusion campaigns underlining the fact that this phenomenon is not an artifact. The threshold for the beginning of the main PLS phase separation (depercolation) is less marked than for oxygen. This is probably due to starch plasticization (by water swelling) which could activate the water transport in blends with high PLS contents.

As a conclusion, depending on the relevant choice of the probes, permeation of small probe molecules is a rapid tool complementary to solvent extraction and microscopic observations to get additional information on the morphology of immiscible polymer blends with phases differing in their permeation properties as in the present case. Results are in very good agreement with previous collected data (continuity diagram and microscopic observations), and it is now clear that the continuity curve obtained for starch in Fig. 1 is rather accurate and that the short ultimate step of thermoforming performed to get constant materials thickness for transport studies does not seem to modify significantly the morphology of blends.

3.2.2. Water vapor sorption experiments

The determination of water sorption properties (water uptake and kinetics) gives information on PLS phase availability for water. More specifically, it was here interesting to disconnect the thermodynamic effects (water solubility) from the kinetic ones (diffusion) as they are merged in the water permeation study. Fig. 4 shows the water content at equilibrium at 45% and 75% RH at 20 °C for the different blends. As expected, PLS (polar polymers) and PBSA (semi-polar polymers) have a very different intrinsic water uptake at 75% RH: more than 30 wt.% water uptake against less than 1 wt.%, respectively.

Up to 11 films were used simultaneously to minimize the sampling scattering and to record significant amounts of water. In Fig. 4, the results are compared with the theoretical ones (dotted lines) according to the mixing law, taking into account the contribution of the experimental water uptakes of each component. As expected, the addition of PBSA decreases the water uptake of the blends at equilibrium as PBSA is less hydrophilic than PLS. At low RH (45%),

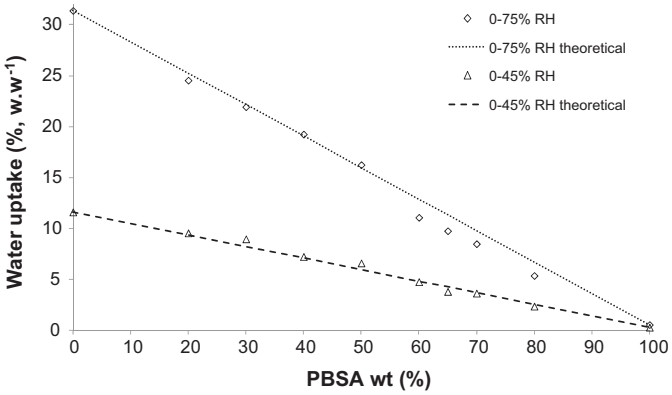

Fig. 4. Water uptake at 45% and 75%RH (experimental data, dotted lines for the calculated water uptake values at 45% - - - and 75% ····) as a function of PBSA content for PBSA/PLS films.

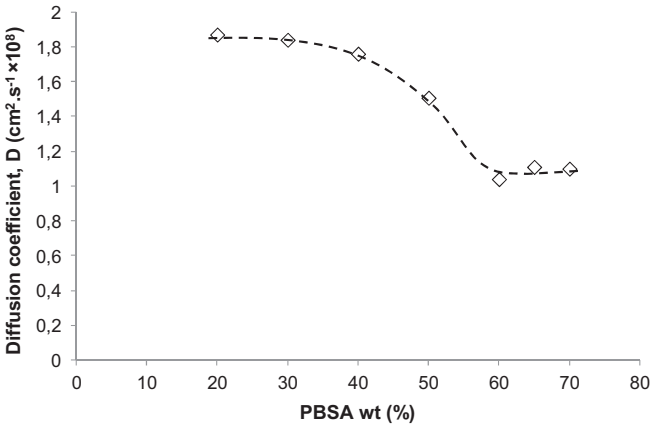

Fig. 5. Apparent diffusion coefficients of water in PBSA/PLS blends versus PBSA content.

experimental and theoretical data are superimposed: experimental values can be well predicted by the mixing law. At higher RH (75%), experimental data at high PBSA contents (from PBSA60 to PBSA80) are lower than the predicted ones. This discrepancy corresponds to the beginning of the PBSA phase continuity in the blends (beginning when PBSA composition of blends exceeded 55%). These results can be explained by the limited swelling of PLS nodules entrapped in a continuous PBSA phase (Belard, Dole, & Avérous, 2009). Unfortunately, it was not possible to make measurements at higher RH values (>75%) to study higher swelling degree as glycerol exudation was observed for such plasticized films and perturbed the analysis.

Fig. 5 presents the apparent water diffusion coefficient (D_{water}) versus PBSA content, obtained for a water vapor partial pressure increment corresponding to a RH increase from 45% to 75% RH at 20 °C. D_{water} for PBSA 80 was not calculated as a time lag was observed (Eq. (2) not applicable). D_{water} decreases with addition of PBSA to remain nearly constant beyond 60% of PBSA (Fig. 5). This phenomenon occurs progressively when diffusing paths increase in tortuosity until PBSA forms a continuous phase: D_{water} remains then constant (i.e. above 55% (Fig. 1) or 60% (Fig. 5) PBSA content in PLS/PBSA blends). The water sorption kinetics are governed by the blend morphology with an interesting S-shape control.

3.2.3. Desorption study

Blends were formulated with water soluble fluorescein sodium salt mainly located in polar PLS phase as already observed by CSLM (Fig. 2). Films from pure PLS to PBSA80% blends were prepared in order to study the kinetics of fluorescein release into a water bath. This allowed to study the mass transfer of an easily detectable compound of a higher molecular mass (376 g mol^{-1}) than water. As expected, fluorescein release kinetics decrease from PBSA0 to PBSA80 films as shown in Fig. 6. Normalized values are scattered depending probably on the samples homogeneity. However, it is obvious that fluorescein desorption kinetics were governed by the PBSA content in the blends. For PBSA80 blend, a noticeable lag time before fluorescein desorption can be observed.

The apparent diffusion coefficients of fluorescein ($D_{fluorescein}$) in blends can be estimated on the basis of a Fickian behavior: the corresponding values are displayed in Fig. 7. $D_{fluorescein}$ in PBSA/PLS blends gradually decreases with PBSA content up to a plateau value corresponding to a 40% PBSA content in blends when PLS continuity index decreases below 100%. A similar plateau was already observed for water molecules; however, the corresponding PBSA content threshold was higher (60%). The gradual decrease of $D_{fluorescein}$ is probably due to the increase of the tortuosity of the PLS phase paths crossing the PBSA/PLS blends when the PBSA content increases. Interestingly, fluorescein delivery is highly dependent on the blends morphology and its release can be controlled by the blend composition.

3.2.4. Discussion on transport properties

Diffusion paths available for water seem to be less selective than those elected by fluorescein. Fluorescein has a higher molecular mass and seems to be able to cross the films only through PLS continuous paths (which appeared in blends containing less than 40% PBSA): a total PLS continuity was thus necessary for fluorescein desorption.

Water vapor could probably cross the PBSA thin barriers: partial continuity is not an actual barrier for water and it is obvious that it is necessary to have a total continuity for PBSA to finally decrease its apparent diffusion coefficient (i.e. 60% PBSA materials).

A simple tortuosity factor (τ) used for diffusion through heterogeneous systems can be calculated from Eq. (4). It corresponds to the ratio of effective paths length e_{eff} (diffusion sinuous path length

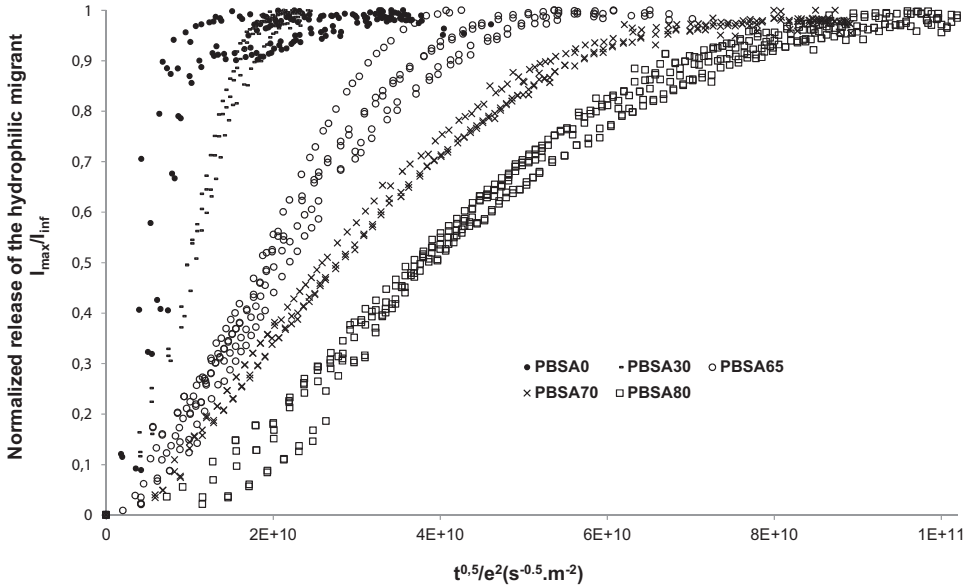

Fig. 6. Fluorescein desorption kinetics from PBSA/PLS blends into water as a function of the blend composition. The intensity ratio corresponds to the percentage of released fluorescein.

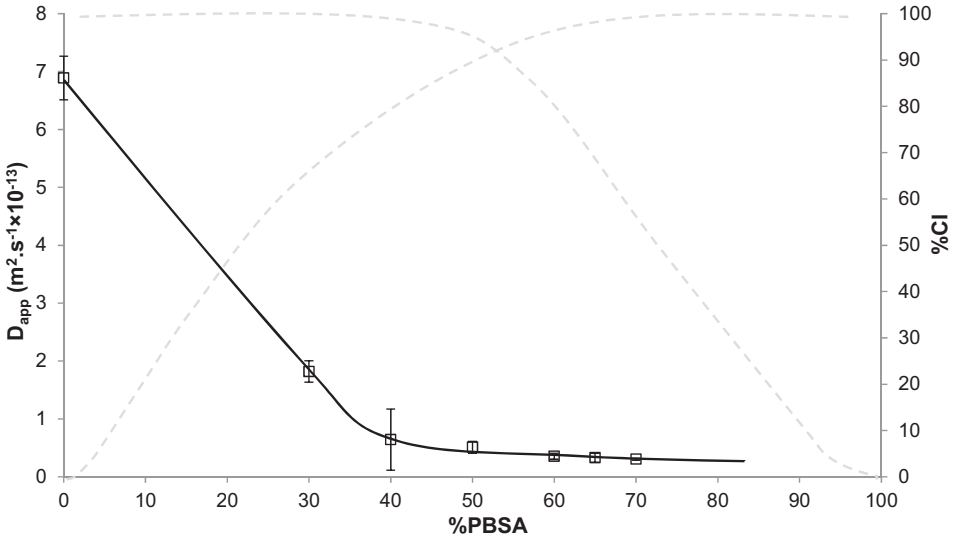

Fig. 7. Apparent diffusion coefficient of fluorescein in PLS/PBSA blends as a function of PBSA content. The PBSA continuity curve from Fig. 1 (dotted line) is added for memory.

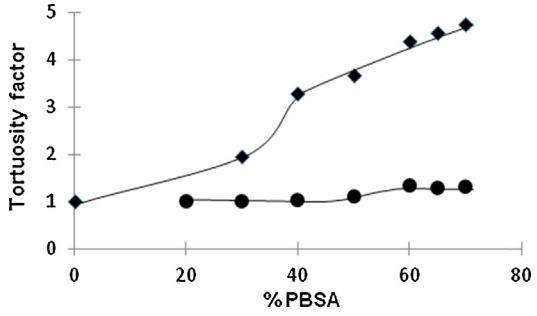

Fig. 8. Calculated tortuosity factor for fluorescein (squares) and water (circles). Lines are only guides for eyes.

assuming that diffusion occurs only in the polar PLS phase for the same D for all blends) to the actual sample thickness e_{ref} (direct length in Eq. (2)).

$$\tau = \sqrt{\frac{D_1}{D_{ref}}} = \frac{e_{eff}}{e_{ref}} \quad (4)$$

D_1 is the apparent diffusion coefficient (Eq. (2)) and D_{ref}, the apparent diffusion coefficients in pure starch materials (fluorescein) or through the blend with the lowest PBSA content (20% PBSA for water sorption). Indeed, D_{ref} is the diffusion coefficient in PLS which should be constant when transport occurs in this phase, whatever the material composition. τ represents thus the multiplying factor to apply to the sample thickness to approximate the effective path length taken by the diffusing molecule. In Fig. 8, this factor is represented as a function of the material composition for water and fluorescein.

As already discussed, fluorescein is much more impacted by the tortuosity factor (path length multiplied up to five times) than water which can partially pass through the thinnest PBSA cluster walls.

4. Conclusion

This paper deals with the morphological study of PBSA/PLS blends for the design of controlled release active materials. Films with distinct morphologies were designed by changing the blend composition. The blend compositions for which each polymer phase forms a continuous phase available for intrinsic diffusion paths were identified: PLS and PBSA phase continuities were observed for blends containing 50–55% PLS and 55–60% PBSA, respectively.

Release was controlled by the diffusion path tortuosity and by the limited swelling of the polar phase. Fluorescein release was clearly more impacted than water by the tortuosity factor tailored by the blend composition. This behavior is promising for the controlled release of polar migrants: it should be possible to extrapolate these results to higher molecular mass molecules, which would take the most tortuous paths to diffuse playing with their specific affinity to one phase of such a biphasic polymer blend. Migrants with higher molecular mass like food preservatives (embedded in packaging materials and/or coatings) could thus present a well controlled release resulting from a tailored tortuous morphology achieved by a relevant polymer blend composition for which the swelling of the polar phase is limited by its entrapment in the other phase.

This study is being continued on such perspectives.

Acknowledgements

The authors would like to thank Dergham Co. Ltd. (Tartus, Syria) for financing the Ph.D. grant of Fadi Khalil, Fonds de Développement de la Recherche (FDR) du technopole Alimentec (Bourg en Bresse, France) for partially funding this project, Dr. Frédéric Prochazka (Laboratoire IMP (Ingénierie des Matériaux Polymères), Université Jean Monnet, Saint Etienne, France) for technical support and fruitful discussions, Annie Perrin and Dr. Patrice Dole (Centre Technique de la Conservation des Produits Agricoles (CTCPA), Bourg en Bresse, France) for oxygen permeation and gas chromatography experiments, advices and comments and Annie Rivoire (CTμ, Lyon, France) for CSLM observations.

Appendix A. Supplementary data

Supplementary data associated with this article can be found, in the online version, at http://dx.doi.org/10.1016/j.carbpol.2014.02.062.

References

Auras, R., Harte, B., & Selke, S. (2004). An overview of polylactides as packaging materials. *Macromolecular Bioscience*, *4*, 835–864.

Averous, L., & Boquillon, N. (2004). Biocomposites based on plasticized starch: Thermal and mechanical behaviours. *Carbohydrate Polymers*, *56*, 111–122.
Belard, L., Dole, P., & Avérous, L. (2009). Study of pseudo-multilayer structures based on starch-polycaprolactone extruded blends. *Polymer Engineering & Science*, *49*, 1177–1186.
Castro, M., Carrot, C., & Prochazka, F. (2004). Experimental and theoretical description of low frequency viscoelastic behaviour in immiscible polymer blends. *Polymer*, *45*, 4095–4104.
Castro, M., Prochazka, F., & Carrot, C. (2005). Co-continuity in immiscible polymer blends: A gel approach. *Journal of Rheology*, *49*, 149–160.
Dole, P., Joly, C., Espuche, E., Alric, I., & Gontard, N. (2004). Gas transport properties of starch based films. *Carbohydrate Polymers*, *58*, 335–343.
Espuche, E., Escoubes, M., Pascault, J. P., & Taha, M. (1999). Transport properties of thermoplastic/thermoset Blends. *Journal Polymer Science: Part B: Polymer Physics*, *27*, 473–483.
Galloway, J. A., Koester, K. J., Paasch, B. J., & Macosko, C. W. (2004). Effect of sample size on solvent extraction for detecting cocontinuity in polymer blends. *Polymer*, *45*, 423–428.
Godbillot, L., Dole, P., Joly, C., Roge, B., & Mathlouthi, M. (2006). Analysis of water binding in starch plasticized films. *Food Chemistry*, *96*, 380–386. http://www.succipack.eu/
Jbilou, F., Joly, C., Galland, S., Belard, L., Desjardin, V., Bayard, R., et al. (2013). Biodegradation study of plasticised corn flour/poly(butylene succinate-co-butylene adipate) blends. *Polymer Testing*, *32*, 1565–1575.
Leuenberger, H., Bonny, J. D., & Kolb, M. (1995). Percolation effects in matrix-type controlled drug release systems. *International Journal of Pharmaceutics*, *115*, 217–224.
Li, J., Ma, P. L., & Favis, B. D. (2002). The role of the blend interface on morphology in cocontinuous polymer blends. *Macromolecules*, *6*, 2005–2016.
Lyu, S. P., Sparer, R., Hobot, C., & Dan, K. (2005). Adjusting drug diffusivity using miscible polymer blends. *Journal of Controlled Release*, *102*, 679–687.
Park, T. G., Cohen, S., & Langer, R. (1992). Poly(L-lactic acid)/pluronic blends: Characterisation of phase separation behaviour, degradation, and morphology and use as protein-releasing matrices. *Macromolecules*, *25*, 116–122.
Pötschke, P., & Paul, D. R. (2003). Formation of co-continuous structures in melt-mixed immiscible polymer blends. *Journal of Macromolecular Science: Part C: Polymer Review*, *43*, 87–141.
Regulation CE no. 1935/2004, CE no. 450/2009.
Rodriguez-Gonzalez, F. J., Ramsay, B. A., & Favis, B. D. (2006). Rheological and thermal properties of thermoplastic starch with high glycerol content. *Enzyme and Microbial Technology*, *39*, 352–361.
Romm, F. (2002). Theories and theoretical models for percolation and permeability in multiphase systems: Comparative analysis. *Advances in Colloid and Interface Science*, *99*(2002), 1–11.
Sarazin, P., Li, G., Orts, W. J., & Favis, B. D. (2008). Binary and ternary blends of polylactide, Polycaprolactone and thermoplastic starch. *Polymer*, *49*, 599–609.
Schwach, E., & Avérous, L. (2004). Starch-based biodegrable blends: Morphology and interface properties. *Polymer International*, *53*, 2115–2124.
Siepmann, F., Siepmann, J., Walther, M., MacRae, R. J., & Bodmeier, R. (2008). Polymer blends for controller release coatings. *Journal of Controlled Release*, *125*, 1–15.
Soney, C. G., Ninan, K. N., & Sabu, T. (2001). Permeation of nitrogen and oxygen gases through styrene-butadiene rubber, natural rubber and styrene-butadiene rubber/natural rubber blend membranes. *European Polymer Journal*, *37*, 183–191.
Song, H., & Lee, S. Y. (2006). Production of succinic acid by bacterial fermentation. *Enzyme and Microbial Technology*, *39*, 352–361.
Woodruff, M. A., & Hutmacher, D. W. (2010). The return of a forgotten polymer-polycaprolactone in the 21st century. *Progress in Polymer Science*, *35*, 1217–1256.
Yu, L., Dean, K., & Li, L. (2006). Polymer blends and composites from renewable resources. *Progress in Polymer Science*, *31*, 576–602.